

A General, Synthetic Model for Predicting Biodiversity Gradients from Environmental Geometry

Kevin Gross^{1,*} and Andrew Snyder-Beattie^{1,2}

1. Biomathematics Program, North Carolina State University, Raleigh, North Carolina 27695; 2. Future of Humanity Institute, Oxford Martin School, University of Oxford, Oxford OX1 1PT, United Kingdom

Submitted August 10, 2015; Accepted May 18, 2016; Electronically published August 9, 2016

Online enhancements: appendix, supplemental material, computer code.

ABSTRACT: Latitudinal and elevational biodiversity gradients fascinate ecologists, and have inspired dozens of explanations. The geometry of the abiotic environment is sometimes thought to contribute to these gradients, yet evaluations of geometric explanations are limited by a fragmented understanding of the diversity patterns they predict. This article presents a mathematical model that synthesizes multiple pathways by which environmental geometry can drive diversity gradients. The model characterizes species ranges by their environmental niches and limits on range sizes and places those ranges onto the simplified geometries of a sphere or cone. The model predicts nuanced and realistic species-richness gradients, including latitudinal diversity gradients with tropical plateaus and mid-latitude inflection points and elevational diversity gradients with low-elevation diversity maxima. The model also illustrates the importance of a mid-environment effect that augments species richness at locations with intermediate environments. Model predictions match multiple empirical biodiversity gradients, depend on ecological traits in a testable fashion, and formally synthesize elements of several geometric models. Together, these results suggest that previous assessments of geometric hypotheses should be reconsidered and that environmental geometry may play a deeper role in driving biodiversity gradients than is currently appreciated.

Keywords: biological diversity, environmental geometry, mathematical model, niche, species range, species richness.

Introduction

Biological diversity gradients fascinate ecologists. Global latitudinal diversity gradients (LDGs) are one of the most pervasive, conspicuous, and ancient characteristics of life (Pianka 1966; Crame 2001; Hillebrand 2004; fig. 1A–1C). Decades of research have identified more than 30 potential mechanisms that may contribute to these gradients (Lomolino et al. 2010; Brown 2014), including ecological (Willig

et al. 2003), evolutionary (Jablonski et al. 2006), and historical (Mittelbach et al. 2007) hypotheses. Elevational diversity gradients (EDGs; often, but not always, along mountainsides) are both more numerous and more varied than LDGs (fig. 1D–1F), and they most frequently show either a steady decline in species diversity as elevation increases or a mid-elevation diversity peak (Rahbek 2005). Hypotheses to explain EDGs largely parallel the explanations proposed for LDGs (McCain and Grytnes 2010).

One class of hypotheses for diversity gradients suggests that LDGs and EDGs arise in part as a consequence of the geometry of the abiotic environment. Two such hypotheses inspire this article. First, in the context of LDGs, Terborgh (1973) and Rosenzweig (1995), among others, have argued that the tropics are more biologically diverse because they comprise a greater contiguous area than any other ecoregion. The tropics possess a greater contiguous area because parallels of latitude are longest at the equator, because the tropical regions of the Northern and Southern Hemispheres form one contiguous climate belt (while both temperate and polar regions of the two hemispheres are disjunct), and because the latitudinal gradient in temperature is nonlinear, such that average temperature changes more rapidly with latitude at high latitudes than at low latitudes. Following Willig et al. (2003), we refer to this as the geographic-area hypothesis. Gorelick (2008) provided the first (and, to the best of our knowledge, only) partial mathematical formalization of the geographic-area hypothesis, but his model captured only the greater area of the tropics, and ignored the effects of their contiguity and the nonlinear temperature gradient.

In a separate vein, others have suggested that Earth's geometry promotes LDGs by constraining the possible placement of species ranges (Colwell and Hurlt 1994; Willig and Lyons 1998; Lees et al. 1999; Colwell and Lees 2000). This “mid-domain effect” (MDE) suggests that when species ranges are placed randomly within a bounded domain, the overlap of species ranges—and hence biological diversity—will be

* Corresponding author; e-mail: kevin_gross@ncsu.edu.

ORCID: Gross, <http://orcid.org/0000-0001-5612-7519>.

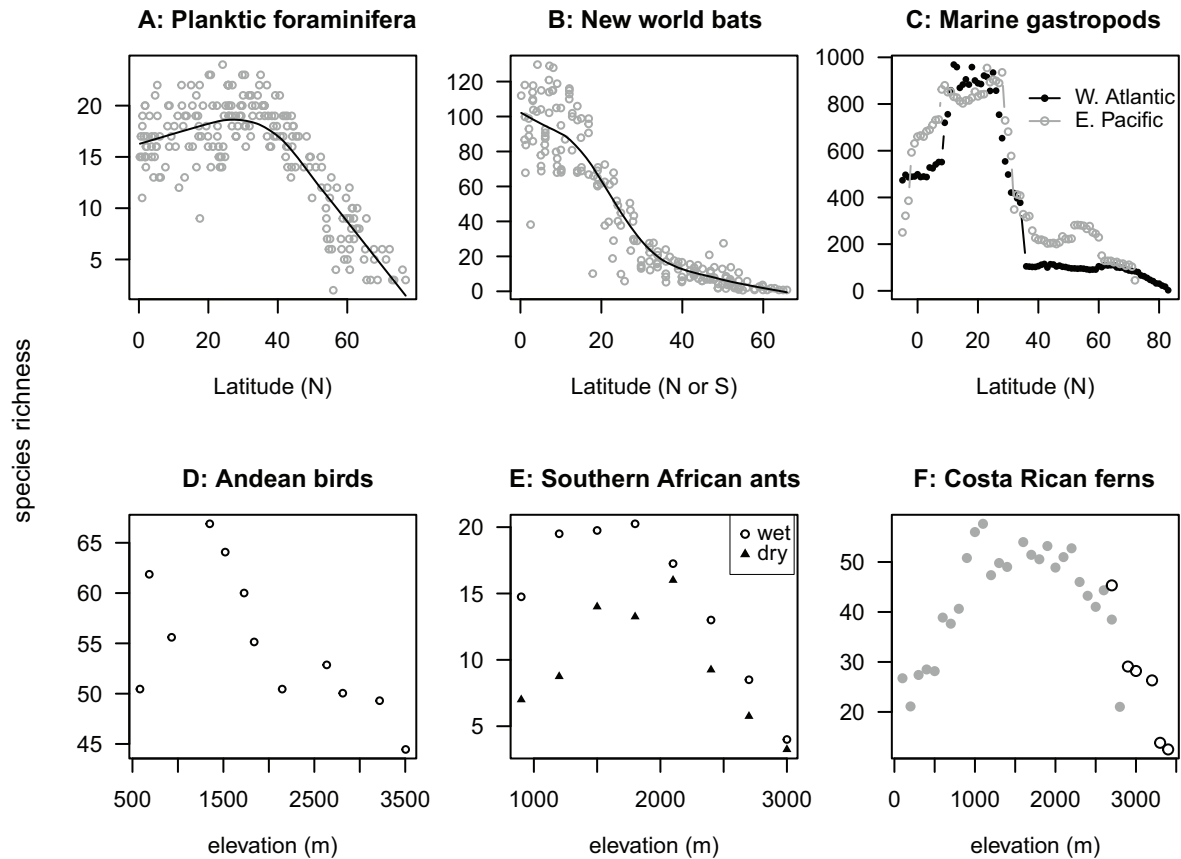


Figure 1: Examples of latitudinal (A–C) and elevational (D–F) biodiversity gradients. All vertical axes show local species richness (alpha diversity). *A*, Planktic foraminifera at sites in the North Atlantic, as calculated by Yasuhara et al. (2012). *B*, Bat species in equally sized grid cells in the New World (Willig and Selcer 1989; published data do not distinguish between north and south latitude). *C*, Marine copepod species along the coast of the Americas, based on overlap of species ranges (Roy et al. 1998). *D*, Bird species in samples of 300 mist-netted individuals at several elevations in the Peruvian Andes, as reported by Terborgh (1977), after Rahbek (1995). *E*, Ant species richness from pitfall traps at sites in southern Africa in the 2009 wet and dry seasons (Bishop et al. 2014). *F*, Species of ferns and their allies sampled exhaustively at several elevations in Costa Rica (different plot symbols show two separate transects; Kluge et al. 2006). Smooth fits in *A* and *B* are loess curves. Detailed data descriptions appear in the supplemental material.

greatest near the domain's center and will decline toward the domain's edges. With respect to LDGs, Colwell and Hurtt (1994, p. 557) suggested that the "northern and southern limits of habitable latitudes . . . for a particular group of organisms" provide the necessary boundaries, leading to greatest species richness in the tropics. Willig and Lyons (1998) and Lees et al. (1999) mathematically formalized the MDE on a one-dimensional domain, and mathematical simulations have been used to explore the MDE on more complicated two-dimensional (e.g., Lees et al. 1999; Jetz and Rahbek 2001; Colwell et al. 2009) and three-dimensional (VanDerWal et al. 2008) domains, and on domains with environmental gradients (Connolly 2005; Rangel and Diniz-Filho 2005).

Geographic area (Rahbek 1997) and the MDE (Grytnes and Vetaas 2002; Colwell et al. 2004) have also been offered as hypotheses to explain EDGs, although in this context they often lead to clashing predictions. When area declines with

increasing elevation—as it usually does for published EDGs (McCain 2007), although area-elevation relationships for entire mountain ranges may be more complex (Elsen and Tingley 2015; Bertuzzo et al. 2016)—the area hypothesis predicts that species richness will decline with increasing elevation.¹ Gorelick (2008) again provided a mathematical model for the area hypothesis on a (conical) mountain and suggested that species diversity should decline at either a constant or an accelerating rate as elevation increases. In contrast, the MDE predicts that biological diversity will peak at mid-elevations, with symmetric declines in diversity on either side of the mid-elevation peak (e.g., McCain 2004).

1. McCain (2007) found that area declined with elevation in 26 of 34 published EDGs. However, Elsen and Tingley (2015) showed that surface area declines with increasing elevation in only 32% of mountain ranges worldwide; mid-elevation peaks in area are more common (39% of mountain ranges).

Current support for the geographic area and MDE hypotheses as drivers of EDGs is mixed (Dunn et al. 2007; McCain and Grytnes 2010).

While no single mechanism is likely to be responsible for all biodiversity gradients (Colwell 2011), the geographic area and MDE hypotheses are useful for understanding how environmental geometry contributes to these gradients. However, our ability to evaluate the empirical support for geometric hypotheses is inextricably tied to our understanding of the predictions that those hypotheses make. Toward this end, the absence of a mathematical model that synthesizes all pathways by which environmental geometry can influence diversity gradients hampers attempts to assess the empirical support for those hypotheses. For example, most (though not all) published geometric models for LDGs predict a relationship between latitude and species richness that is quasi-parabolic and concave down and that peaks at the equator (e.g., Willig and Lyons [1998], Lees et al. [1999], and Gorelick [2008]; Connolly [2005] provides a notable exception). Yet many LDGs (e.g., fig. 1A–1C) show a somewhat different qualitative pattern. In the most recent edition of their text, Lomolino et al. (2010) observed that “rather than exhibiting a continuous decline in species density from the equator to the poles, most taxa exhibit a pattern of relatively high, albeit variable, diversity in the tropics marked by a rapid decline through the subtropics and much more modest declines through the higher latitudes” (p. 670). While this mismatch between data and models is interesting, it is hard to know whether it constitutes a strike against the idea that Earth’s geometry contributes strongly to global LDGs, or merely reflects an incomplete expression of that idea in prevailing models.

This article aims to fill this gap by describing a model for biodiversity gradients driven solely by the geometry of latitudinal or elevational environmental variation and ecological limits on species ranges. The model does not merely recapitulate the geographic-area or MDE hypotheses; instead, it builds a new theory from the ideas embodied in both. To enable analytical progress, our model considers the highly simplified settings of a sphere for LDGs and a cone for EDGs (Gorelick 2008). To be sure, a sphere and cone drastically simplify the geography of Earth and a mountain, respectively, but they permit solutions and insight that would otherwise be more challenging. On the sphere, we consider an environment that changes smoothly between equatorial and polar extremes (fig. 2), while on the cone we assume that the environment varies smoothly from the cone’s base to its apex (fig. 3). The model assumes that species ranges are limited by fidelity to an environmental niche (Brown et al. 1996) and by an upper boundary on their size, and it follows others (e.g., Colwell and Hurtt 1994) in equating local species richness (i.e., alpha diversity) with the overlap of species ranges. Importantly, the model assumes that all environments are equally suitable to life, regardless of latitude or elevation. Thus, the model isolates how the geometry of environmental variation and ecological limits on species ranges can generate biodiversity gradients without invoking additional biological mechanisms.

As we will show, this model synthesizes many of the essential predictions for biodiversity gradients made by previous geometric models. However, it also reveals additional fine structure to these gradients that is not readily apparent in prevailing geometric models. Moreover, although a formal confrontation with data is outside the scope of this

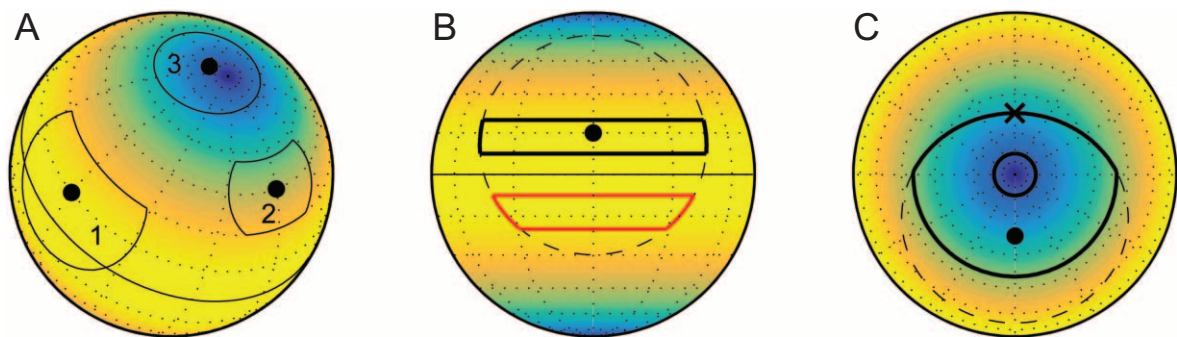


Figure 2: Species ranges on the sphere. Color corresponds to the environmental template $g(x) = 1 - \cos x$, where x is latitude. Solid black lines show range boundaries, and points show range origins. A, Three species ranges. Range 1 encounters an intolerable environment on its northern edge and encounters its maximum radius elsewhere. Range 2 encounters an intolerable environment on both its northern and southern boundaries. Range 3 overlaps a pole, and its boundary is determined entirely by its maximum radius. B, Species ranges must be contiguous. The area outlined in red lies within the range’s maximum radius (shown by the dashed line) and environmental niche but is not part of the range because it is separated from the range origin by intolerable habitat at the equator. C, The range-size limit is measured “as the crow flies.” The dashed line shows the maximum radius. The smaller circle surrounding the pole lies outside the species’ environmental tolerance and is not part of the range. The point indicated by an X lies in the species range, even though all paths that connect it to the range origin while passing through only tolerable habitat are longer than the maximum radius.

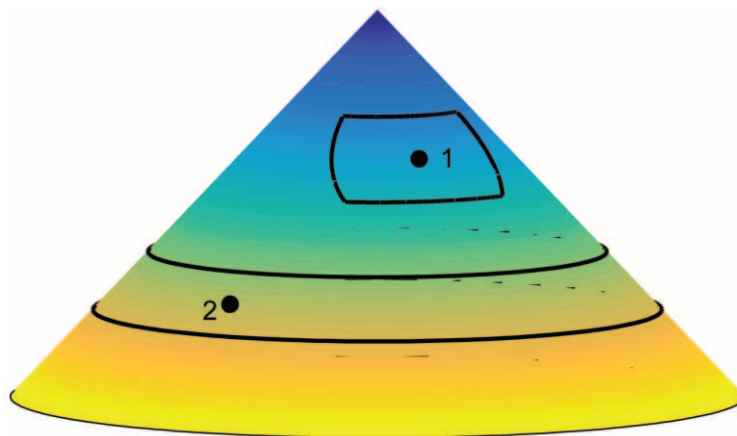


Figure 3: Species ranges on the cone. Color corresponds to the environmental template $g(x) = x$, where x is elevation. Solid black lines show the boundaries of two species ranges, and points show the origins of those ranges. Range 1 is limited by the environment on the upper and lower extents of its range, while its angular extent around the cone is determined by its maximum radius. Range 2 is limited only by its environmental tolerance and thus wraps completely around the cone.

contribution, both the coarse and the fine structure predicted by our model show an intriguing correspondence with empirical biodiversity gradients. Thus, we suggest that previous evaluations of geometric hypotheses for diversity gradients may need to be reconsidered, and that environmental geometry may play a more nuanced role in driving LDGs and EDGs than presently appreciated.

Below we present the basic model structure and key results. Readers interested in a qualitative understanding will want to read the overview subsection of the Methods but can bypass the latter, more technical subsections. An appendix provides mathematical derivations, a PDF includes additional results, a zip file contains computer code, and our technical report (Gross and Snyder-Beattie 2015) presents a deeper mathematical treatment (the appendix, PDF, and zip file are available online).²

Methods

Model Overview

The model begins with a geometry (sphere or cone) onto which species ranges will be placed. An environmental template is then constructed by assigning an environment (in this case, a single numerical value) to every location on the geometry. Species ranges are formed by assigning three characteristics to each range: a location where the range originates, an environmental tolerance, and a maximum radius. Species ranges expand outward from the range origin until they either encounter an environment that differs from the environment at the range origin by more than the environ-

mental tolerance, or are farther away from the range origin, than the maximum radius. The species richness at a location is then taken to be the proportion of all species ranges that overlap that location. This algorithm for constructing species ranges is similar to algorithms devised by Rangel et al. (2007) and Tomašových et al. (2015), who also constructed species ranges via spatial expansion from a range origin and fidelity to an environmental niche.

The model thus assumes that species ranges are limited by the species' environmental tolerance and an upper limit on the range's size. The idea that species ranges are limited by a species' environmental tolerance is well established (Brown et al. 1996). The upper bound on a range's size is a modeling construct intended to capture the many processes that can limit a species range beyond the availability of suitable environments. For example, in a more complex world than the simplified geometries considered here, species ranges are apt to encounter physical (e.g., a land/water interface) or biological (e.g., lack of obligate mutualist partners) boundaries to further dispersal (Brown et al. 1996). In addition, over evolutionary time large species ranges will tend to fracture via speciation (Rosenzweig 1992). Together, these and other processes impose additional limits on the size of species ranges beyond fidelity to an environmental niche; the maximum range radius is meant to encompass these processes.

Thus, the model takes the following parameters: the environmental template and a probability distribution for the triple of range origins, environmental tolerances, and maximum range sizes across species. We assume that range origins, environmental tolerances, and maximum range sizes are distributed independently among species, and we also assume that range origins are distributed uniformly across

2. Code that appears in *The American Naturalist* is provided as a convenience to the readers. It has not necessarily been tested as part of the peer review.

the geometry. Either of these assumptions could easily be modified if, say, environmental tolerance was assumed to differ between tropical and temperate species, or species were assumed to originate more frequently in the tropics (e.g., Fischer 1960; Rohde 1992; Jablonski et al. 2006). In this article, we focus on species richness at a given location (i.e., alpha diversity). We present expressions for the expected alpha diversity as a function of latitude or elevation, although these expressions often must be solved numerically. The model could also be used to predict species richness integrated along a band of latitude or elevation (i.e., gamma diversity), although we do not pursue that aim here.

LDGs on the Sphere

Let $(x, \phi) \in [-\pi/2, +\pi/2] \times (-\pi, +\pi]$ be a coordinate system on the unit sphere, where x is latitude and ϕ is longitude. Let $g(x) \in [0, 1]$ be a function that gives the environment for each latitude. (The environment is not affected by longitude.) We assume that the environment is symmetric with respect to the equator ($g(x) = g(-x)$) and varies smoothly between equatorial and polar extremes. (Technically, $g(x)$ is continuous and strictly monotonic on $x > 0$; without loss of generality, we assume $g(0) = 0$, $g(\pi/2) = 1$, and $dg/dx > 0$ for $x > 0$.) Let $g^{-1}(\cdot) \geq 0$ be the function that gives the (northern) latitude for a given environment.

Let $\gamma \in [0, 1]$ denote a species' environmental tolerance. A species range that originates at (x_o, ϕ_o) can include only locations where the environment differs from $g(x_o)$ by no more than γ . That is, the species range will be a subset of $\mathcal{E} = \{(x, \phi) : |g(x) - g(x_o)| \leq \gamma\}$, the collection of all locations within a species' environmental niche. Larger values of γ yield wider niches, all else being equal.

Let $\delta \in [0, \pi]$ denote a the maximum radius of a species' range. Let $d((x_1, \phi_1), (x_2, \phi_2))$ denote the great-circle distance between two points. A species range will also be a subset of $\mathcal{D} = \{(x, \phi) : d((x_o, \phi_o), (x, \phi)) \leq \delta\}$, the collection of locations that lie within a distance δ of a range origin.

Given a range origin (x_o, ϕ_o) , an environmental tolerance γ , and a maximum radius δ , we define the species range as the contiguous subset of the intersection $\mathcal{E} \cap \mathcal{D}$ that contains the range origin (fig. 2A). We require that the range be contiguous to avoid species ranges with separate, noncontiguous territories (which would otherwise be possible near the equator; fig. 2B; Tomašovych et al. 2015). This definition captures the essential features of our model while remaining analytically tractable. It is worth noting, however, that the range-size limit is applied "as the crow flies" and thus may pass over intolerable environments; it is not restricted to paths that pass through only tolerable environments (fig. 2C). Arguably, it might be more compelling to require a point in a species range to connect to the range origin by a path no longer than δ that lies entirely within

\mathcal{E} , but this definition is mathematically cumbersome. Spreading dye models (Gotelli and Graves 1996) may be better able to accommodate this definition, but such models are beyond the scope of this article.

To develop ideas, we momentarily assume that all species have the same environmental tolerance γ and the same maximum radius δ . Let $S(x, \phi; \gamma, \delta)$ denote the proportion of these species found at the point (x, ϕ) . Because species richness in our model does not depend on longitude, we write $S(x; \gamma, \delta)$, although we emphasize that this is the species richness at any point on the parallel at x (alpha diversity); it is not the total species richness integrated over the entire parallel (gamma diversity). Species richness will be the same in the Northern and Southern Hemispheres (e.g., $S(x; \gamma, \delta) = S(-x; \gamma, \delta)$), so without loss of generality we consider $x \geq 0$. It is helpful to write S as the sum of two components $S_0(x; \gamma, \delta)$ and $S_1(x; \gamma, \delta)$, which give the species richness resulting from ranges that originate on the same or the opposite side of the equator as x , respectively.

First consider $S_0(x; \gamma, \delta)$. To be concrete, consider species richness at the point $(x, \phi = 0)$. To find S_0 , we need to integrate the density of species origins $f(x, \phi)$ over the region defined as follows: a species range originating from any point in the region would overlap $(x, 0)$.³ This integral takes the form

$$S_0(x; \gamma, \delta) = \int_{L(x)}^{U(x)} \int_{-\phi_y}^{\phi_y} f(y, \phi) d\phi dy, \quad (1)$$

where y and ϕ are variables of integration. The outer integral of equation (1) is with respect to latitude, where the bounds of integration $0 \leq L(x) \leq U(x) \leq \pi/2$ give the lower- and uppermost latitudes of origins whose ranges can reach $(x, 0)$. The inner integral of equation (1) is with respect to longitude. For a latitude $y \in [L(x), U(x)]$, $\phi_y \in [0, \pi]$ is the easternmost longitude from which a range can reach $(x, 0)$. By symmetry, $-\phi_y$ is the corresponding westernmost longitude. In the appendix, we show that $L(x)$ and $U(x)$ are given by

$$\begin{aligned} L(x) &= (x - \delta) \vee g^{-1}((g(x) - \gamma) \vee 0), \\ U(x) &= (x + \delta) \wedge g^{-1}((g(x) + \gamma) \wedge 1), \end{aligned} \quad (2)$$

where $a \vee b = \max(a, b)$ and $a \wedge b = \min(a, b)$. For a heuristic understanding of equation (2), consider the formula for $L(x)$. The quantity $x - \delta$ provides for the maximum radius, and the quantity $g^{-1}((g(x) - \gamma) \vee 0)$ provides for the environmental tolerance. $L(x)$ is then the latitude closest to x that satisfies both criteria. The formula for $U(x)$ is constructed similarly. Also in the appendix, we use the formula for the

3. The region of integration may seem unnecessarily convoluted—why not just integrate instead over the range of a species originating at $(x, 0)$? While such an approach would work in some cases—including S_0 on the sphere and S on the cone—it does not work everywhere, including for S_1 on the sphere. For more details, see Gross and Snyder-Beattie (2015).

great-circle distance between two points on the surface of a sphere to show that ϕ_y is given by

$$\phi_y = \cos^{-1} \left[-1 \vee \frac{\cos \delta - \sin x \sin y}{\cos x \cos y} \right]. \quad (3)$$

See figure A1 (figs. A1, A2 are available online) for an illustration.

To derive $S_1(x; \gamma, \delta)$, we again consider the location $(x, 0)$ without loss of generality. We seek an integral of the form

$$S_1(x; \gamma, \delta) = \int_{U_1(x)}^{L_1(x)} \int_{-\phi_y}^{\phi_y} f(y, \varphi) d\varphi dy. \quad (4)$$

In equation (4), the outer bounds of integration $-\pi/2 \leq U_1(x) \leq L_1(x) \leq 0$ are the parallels of latitude farthest from and closest to the equator, respectively, from which a range can originate and overlap $(x, 0)$ (fig. A1). In the appendix, we show that these bounds are given by

$$\begin{aligned} U_1(x) &= -g^{-1}(\gamma) \vee (x - \delta), \\ L_1(x) &= -g^{-1}(0 \vee (g(x) - \gamma)). \end{aligned} \quad (5)$$

It is not guaranteed that $U_1(x) < L_1(x)$; if $U_1(x) \geq L_1(x)$, then $S_1 = 0$. For $y \in [U_1(x), L_1(x)]$, ϕ_y in equation (4) is again given by equation (3).

Finally, we relax the assumption that all species have the same environmental tolerances and range-size limits. We place probability densities $f(\gamma)$ on γ and $f(\delta)$ on δ and integrate over these densities to give $S(x)$, the species richness as a function of latitude:

$$S(x) = \iint S(x; \gamma, \delta) f(\gamma) f(\delta) d\delta d\gamma, \quad (6)$$

where $S(x; \gamma, \delta) = S_0(x; \gamma, \delta) + S_1(x; \gamma, \delta)$.

EDGs on the Cone

Following Gorelick (2008) and Colwell and Rangel (2010), we use a right circular cone as a simplified geometry for an isolated mountain. (See Elsen and Tingley [2015] and Bertuzzo et al. [2016] for recent evidence that a cone may not capture the elevational distribution of some terrestrial mountain ranges, especially those shaped by fluvial erosion. Adaptation of our model to more complex and realistic topographies awaits future work.) A cone with an environment that changes smoothly with elevation has a topology similar to a hemisphere with an environment that changes smoothly with latitude (fig. 3). Thus, species richness on the cone can be derived similarly to S_0 on the sphere, after suitable changes are made to the coordinate system and distance function. The coordinates for a cone are $(x, \phi) \in [0, 1] \times [-\pi, +\pi]$, where x is the position along a base-to-apex transect on the cone's surface, with $x = 0$ corresponding to the

base and $x = 1$ corresponding to the apex. The coordinate ϕ is the compass direction with respect to east, although in our model species richness depends only on elevation.

In the interest of brevity, we relegate the full model for the cone to the appendix. In the main text, we focus on a special case where species ranges are not limited by a maximum size. Our motivation is that the spatial scale of EDGs (10^{-1} – 10^2 km) is likely to be considerably smaller than the spatial scale of LDGs (10^3 – 10^4 km; Rahbek 2005). On these smaller spatial scales, processes that limit range size beyond environmental niche fidelity are apt to be less important in determining species ranges. In this special case, if species origins are distributed uniformly across the surface of the cone, then the proportion of species with environmental tolerance γ that overlap a location with elevation x is given by

$$S(x; \gamma) = (1 - L(x))^2 - (1 - U(x))^2, \quad (7)$$

where $L(x)$ and $U(x)$ are the lowest and highest elevations from which a range can originate and reach elevation x (derivation of eq. [7] is given in the appendix). $L(x)$ and $U(x)$ can be derived similarly to equation (2), giving $L(x) = g^{-1}((g(x) - \gamma) \vee 0)$ and $U(x) = g^{-1}((g(x) + \gamma) \wedge 1)$. If environmental tolerances take a distribution $f(\gamma)$ across species, then we can integrate $S(x; \gamma)$ over this distribution to give $S(x)$, the species richness as a function of elevation:

$$S(x) = \int S(x; \gamma) f(\gamma) d\gamma. \quad (8)$$

Note that when ranges are not limited by a maximum size, the species richness at a given location with elevation x (alpha diversity) and total richness along a ring at elevation x (gamma diversity) are identical. The steepness of the cone factors into the calculation of $S(x)$ only when ranges are limited by size as well as by environment (appendix).

Results

In the results that follow, we assume that range origins are uniformly distributed across the surface of the sphere or cone.⁴ Thus, resulting biodiversity gradients arise solely from the interplay between the geometry of the abiotic environment and the ecological limits on species ranges. We model variation in those ecological limits (the environmental tolerance, γ , and the maximum radius, δ) by assigning them a beta distribution with the first shape parameter (commonly written as α) equal to 1 and the second shape parameter (commonly β) ≥ 1 . (In the case of δ on the sphere, the beta distribution is placed on δ/π , so that δ ranges

4. The uniform densities are $f(x, \phi) = (1/4\pi) \cos x$ on the sphere and $f(x, \phi) = (1 - x)/(\pi \sin \alpha)$ on the cone, where α is the opening angle of the cone.

from 0 to π .) When $\beta = 1$, this gives a uniform distribution. When $\beta > 1$, the distribution becomes more skewed toward small values, with the probability density having a mode at 0 and declining monotonically toward larger values (fig. A2 illustrates this). These skewed distributions generate many small ranges and few large ones, consistent with patterns often found in range-size data (Gaston 1996). The mean of this beta distribution is $1/(1 + \beta)$.

LDGs on the Sphere

On a sphere, we use the environmental template $g(x) = 1 - \cos x$ to capture latitudinal variation in temperature and associated aspects of the abiotic environment. (We use $1 - \cos x$ instead of $\cos x$ so that $dg/dx > 0$ for $x > 0$; but $g(x) = \cos x$ yields identical results.) Figure 4 shows species richness ($S(x)$) versus latitude (x) for several different distributions of environmental tolerance (γ) and maximum range size (δ) among species. Additional results for other distributions of γ and δ are shown in figures S1 and S2 (available online). Because species richness for one hemisphere (North-

ern or Southern) is the mirror image of the other, only one hemisphere is shown.

Most coarsely, the model generates a negative correlation between latitude and species diversity. While this may not seem remarkable, we emphasize that in this model greater species diversity arises at low latitudes solely as a consequence of the geometry of the environmental template and the ecological assumptions of environmental niche fidelity and upper limits on range sizes. Closer inspection of predicted LDGs reveals a variety of finer structure. We describe these features moving from low to high latitudes. First, there is a plateau of high and relatively constant species diversity in the tropics. This plateau extends farther into the subtropics when species ranges can be large and environmental niches are broad (fig. 4A). When the maximum range size is large, species diversity actually increases gradually as one moves from the equator to nearby low latitudes, leading to a subtle valley in species diversity around the equator (fig. 4A, 4D). Species richness then declines through mid-latitudes, with swifter declines in diversity when environmental niches are narrow. This mid-latitude decline

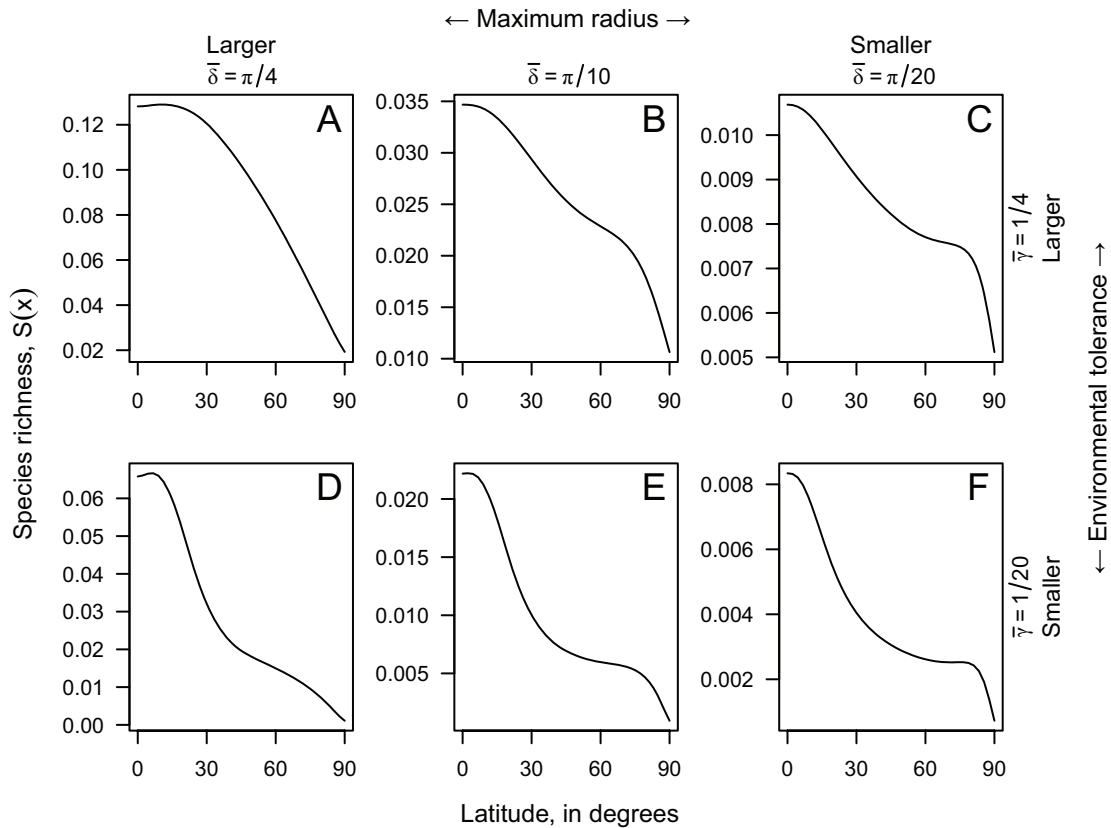


Figure 4: Species richness ($S(x)$) versus latitude (x) for different distributions of the maximum range radius (δ , columns) and the environmental tolerance (γ , rows). Distributions for δ and γ are beta distributions with the first shape parameter equal to 1 and are indicated by their mean values (see text). Note the difference in vertical scales among panels.

in species diversity is often punctuated by an inflection point, above which species diversity declines more slowly as latitude increases (e.g., fig. 4B–4F). When range-size limits are strong and environmental niches are narrow, a second diversity plateau appears at mid- to high latitudes (fig. 4C, 4E, 4F).⁵ When this second plateau exists, though, it terminates in a steep drop in species diversity near the poles.

The geographic-area hypothesis suggests that Earth's geometry influences LDGs through three distinct pathways: low-latitude environments are more abundant, the tropics are compact, and latitudinal temperature gradients are nonlinear (Terborgh 1973; Rosenzweig 1995). All of these mechanisms would suggest that species diversity should peak at the equator. However, in this model these three mechanisms exist in tension with a fourth: both equatorial and polar environments are extreme, while mid-latitude environments occur in the middle of the environmental spectrum. Thus, mid-latitude environments fall within the environmental niche of more species than the extreme environments of the poles or equator. This mid-environment effect counters the effects of geographic area and increases species richness at mid-latitudes. This effect has been observed before (Brayard et al. 2005; Carranza et al. 2008; Letten et al. 2013; Tomašových et al. 2015), although this model is the first to integrate it formally with the geographic-area hypothesis.⁶

Figure 5 illustrates how the three elements of the geographic-area hypothesis and the mid-environment effect combine to generate LDGs. Figure 5A and 5B shows LDGs with an environment that changes linearly with latitude ($g(x) = |2x/\pi|$) and with an imaginary range-truncating barrier at the equator. In this scenario, the greater abundance of low-latitude environments and the mid-environment effect are the primary mechanisms by which environmental geometry impacts biodiversity.⁷ Perhaps surprisingly, species richness peaks at mid-latitudes in these scenarios, suggesting that the effect of greater abundance of low-latitude environments is weak compared with the mid-environment effect. The mid-environment effect is stronger when species can tolerate a broad range of environments (fig. 5A) and is

weaker when environmental niches are narrow (fig. 5B). Removing the range boundary at the equator (but maintaining the linear environment) adds the effect of the compactness of the tropics. This effect greatly increases species diversity at low latitudes, but LDGs continue to display a pronounced valley in species richness at the equator (fig. 5C, 5D). Finally, changing to a nonlinear environment introduces the effect of the shallow temperature gradient at the tropics. This increases species richness at low latitudes even further, thus yielding plateaus in species richness at the tropics coupled with mid-latitude declines in diversity (fig. 5E, 5F).

The occasional secondary plateau in species richness at high latitudes under some scenarios (e.g., fig. 4E, 4F) is surprising and has not been found in previous geometric models. This high-latitude plateau arises as a balance of several different effects. First, because meridians of longitude converge at higher latitudes, the longitudinal extent of species ranges increases at an accelerating rate as one moves toward the poles. All else being equal, this tends to increase diversity at high latitudes. At the same time, however, three mechanisms decrease diversity at high latitudes: parallels of latitude become shorter (leading to fewer species with high-latitude niches, if range origins are uniformly distributed), the nonlinear environmental gradient becomes increasingly steep, and the longitudinal extent of a range cannot increase any farther once the range completely encircles the pole (e.g., fig. 2C). High-latitude diversity plateaus occur when these forces roughly balance. Eventually, however, the latter three effects predominate, and species diversity drops near the poles. Figure S3 illustrates this phenomenon.

EDGs on the Cone

On the cone, we study an environment that changes linearly with elevation, that is, $g(x) = x$. This is reasonable if the abiotic environment is governed primarily by temperature, which generally decreases linearly with increasing elevation on mountains (Barry 2008; McCain and Grytnes 2010). Figure 6 shows species diversity versus elevation for several distributions of environmental tolerances. As a reminder, these results are for the special case when species ranges are not limited by a maximum size and thus wrap completely around the cone. In all cases, species richness peaks closer to the base of the cone than its apex. These EDGs arise from a tension between two of the four mechanisms that drive LDGs on a sphere. On the one hand, mid-elevation environments can be tolerated by the broadest collection of species, promoting a hump-shaped relationship between species richness and elevation. On the other hand, low-elevation environments are more abundant on a cone. Thus, if range origins are uniformly distributed, then there are more species with low-elevation niches. The balance between these two forces yields a hump-shaped EDG with di-

5. Indeed, under some parameterizations a secondary peak in species richness occurs at high latitudes; see figures S1 and S2.

6. What we refer to as a mid-environment effect, Brayard et al. (2005), Carranza et al. (2008), and Letten et al. (2013) refer to as an MDE along an environmental axis. In this article, we find it cleaner to reserve the term "mid-domain effect" for a bounded spatial or geographic domain and use "mid-environment effect" as a term that references (and pays homage to) the MDE, while distinguishing between bounded geographic domains versus dimensions of environmental variation.

7. The addition of a range-truncating boundary at the equator also introduces an MDE that increases species richness at the pole (the midpoint of the hemisphere). As figure 5A and 5B suggests, this effect is weak, and it vanishes when the imaginary equatorial boundary is removed. Thus, we do not dwell on it here.

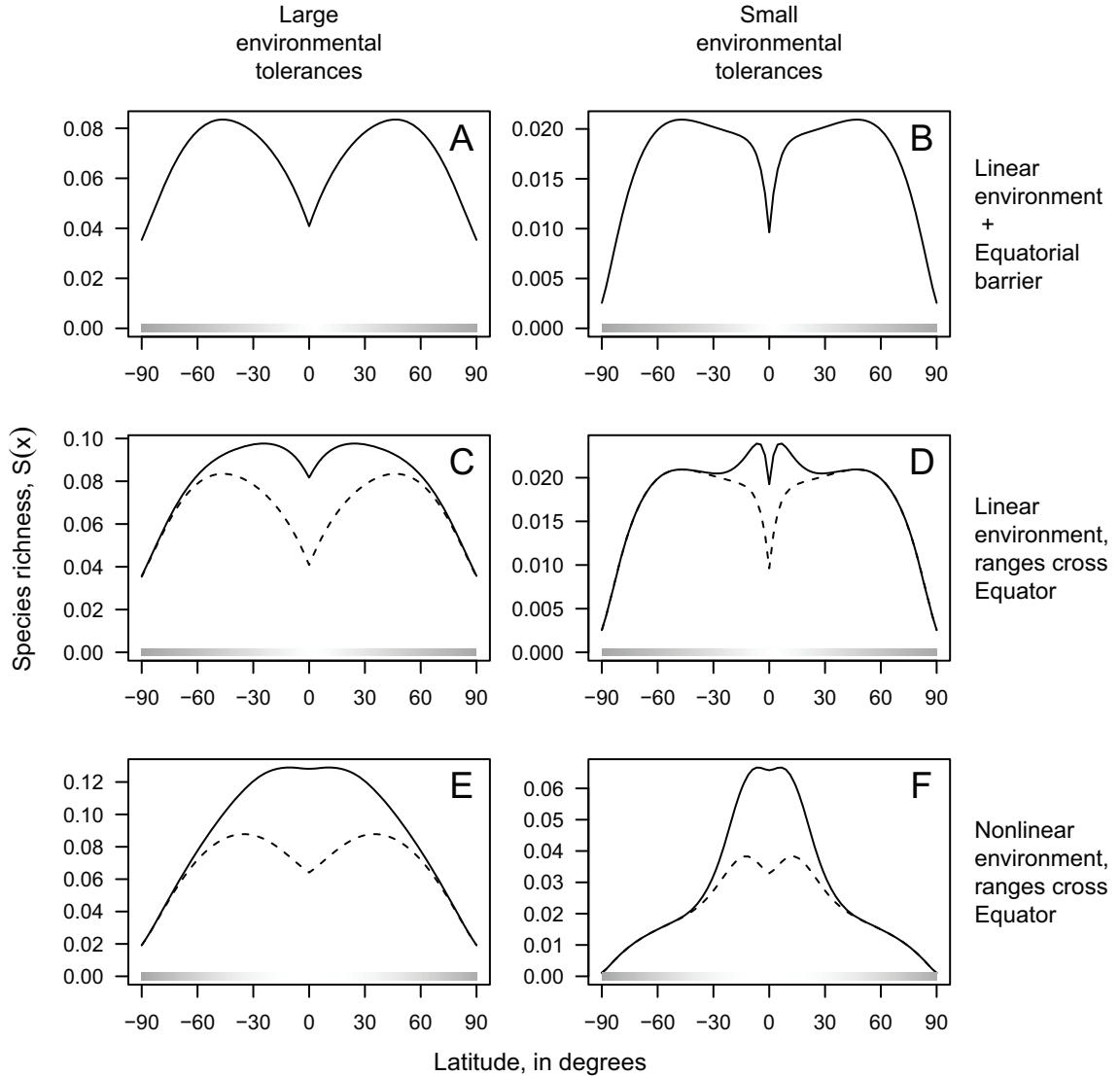


Figure 5: Environmental geometry impacts latitudinal diversity gradients (LDGs) through four different pathways. *A, B*, Species richness $S(x)$ versus latitude (x) on a sphere with a linear environmental gradient and a range-truncating barrier at the equator. These LDGs include the effects of a greater abundance of tropical environments and a mid-environment effect. *C, D*, LDGs on a sphere with a linear environmental gradient and species ranges that can cross the equator. These LDGs add the effect of the compactness of the tropics to the LDGs in *A* and *B*. *E, F*, LDGs on a sphere with a nonlinear (cosine) environmental gradient and species ranges that can cross the equator. These LDGs add the effect of the nonlinear environmental gradient to the LDGs in *C* and *D*. In the left column, the average environmental tolerance across species is $\bar{\gamma} = 1/4$; in the right column, $\bar{\gamma} = 1/20$. The average maximum radius is $\bar{\delta} = \pi/4$ throughout. Grayscale bars depict the environmental gradient. Dashed lines in *C–F* show $S_0(x)$, the species richness when species ranges cannot cross the equator. *E* and *F* correspond to figure 4A and 4D, respectively.

versity peaking below the gradient's midpoint. As species' environmental tolerances become more limiting, the mid-environment effect becomes less important, and the peak in species richness moves closer to the cone's base.

Figure S4 shows additional results for the cone that include a limit on the maximum range size. In brief, strong limits on range size reduce the importance of the unequal

distribution of environments, leading to a peak in species richness at higher elevations.

Discussion

These results show how the interplay among environmental geometry, niche fidelity, and upper limits on range size

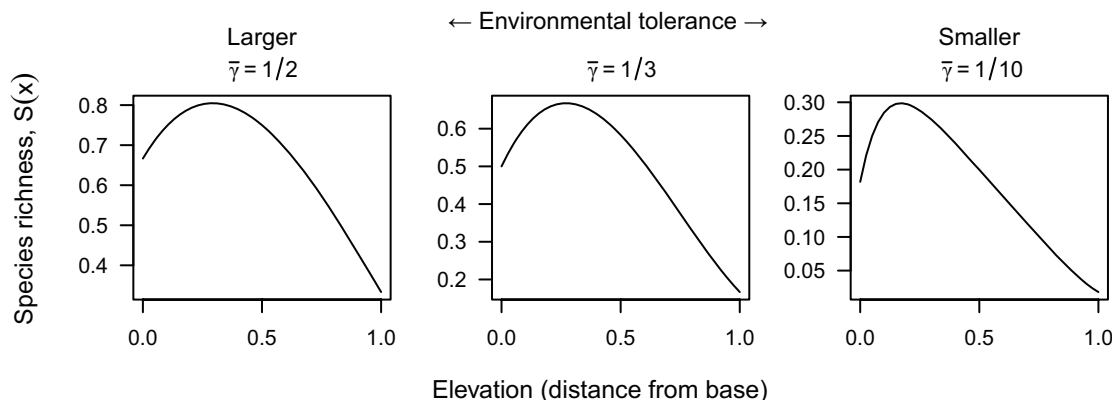


Figure 6: Species richness ($S(x)$) versus elevation (x) on a cone, where only the environmental tolerance limits species ranges. Environmental tolerances (γ) take a beta distribution with means $\bar{\gamma} = 1/2, 1/3$, or $1/10$.

can yield a surprisingly rich variety of latitudinal and elevational biodiversity gradients. These predicted diversity gradients synthesize elements of earlier work and identify some additional fine structure that previous geometric models have not anticipated. Moreover, model exploration suggests how the features of these predicted gradients are modulated by ecological traits and thus provides grist for future empirical evaluation. These insights sharpen our ability to resolve the impacts of the many drivers—both geometric and otherwise—that combine to generate the diversity gradients that typify life (Colwell 2011).

On a sphere, this model predicts LDGs with more complex structure than the quasi-parabolic relationship between latitude and species richness predicted by other analytic geometric models (Willig and Lyons 1998; Lees et al. 1999; Gorelick 2008). Prominent features of this structure include broad plateaus in diversity at low latitudes, subtle equatorial valleys in species richness when environmental niches are narrow and other limits on range size are weak, mid-latitude inflections where the loss of diversity slows with increasing latitude, and occasional secondary plateaus in species richness at mid- to high latitudes, especially when environmental niches are narrow. Although a formal confrontation with data awaits future work, the concordance between several of these predictions and documented LDGs is striking (e.g., fig. 1A–1C). Indeed, Lomolino et al.'s (2010) textbook characterization of LDGs (quoted in the introduction) matches the qualitative predictions of our model nearly to a tee and suggests that environmental niches are on the narrow side of those explored here (e.g., fig. 4D–4F).

Some of the more surprising predictions of this model for LDGs are occasional equatorial diversity valleys and high-latitude diversity plateaus. In the model, equatorial valleys in species richness arise from a tension between a mid-environment effect, which promotes greater species richness at mid-latitudes, and the three elements of the geographic-

area hypothesis (Terborgh 1973), each of which promotes greater species richness at the equator. (Fig. S5 provides a visual explanation of this phenomenon.) Comparable equatorial diversity valleys were also found in the “geophyletic” (i.e., geographic and evolutionary) model of Brayard et al. (2005) and arose from a somewhat similar mechanism.⁸ Brayard et al.'s (2005) model was inspired by LDGs of Atlantic planktic foraminifera, a taxon for which diversity gradually increases from the equator to the subtropics before declining sharply beyond approximately 30°N (Rutherford et al. 1999; Yasuhara et al. 2012; fig. 1A). Equatorial diversity valleys are well documented for oceanic taxa; Tittensor et al. (2010) observed that most oceanic taxa peak in richness between 20° and 40° latitude. Moreover, Brayard et al. (2005) observed that equatorial valleys in diversity are prominent for a host of marine and terrestrial taxa and questioned the common practice of dismissing these valleys as uninteresting artifacts. Our model adds theoretical support to Brayard et al.'s (2005) suggestion that equatorial diversity valleys may be an underexplored subject worthy of deeper scrutiny and investigation.

The high-latitude diversity plateau predicted by our model has (to the best of our knowledge) not been anticipated by geometric models, perhaps because no prior model captures polar geometry. However, empirical evidence for a secondary high-latitude plateau in species richness is hard to find. Roy et al. (1998) found a secondary peak in marine

8. Brayard et al. (2005) state that their equatorial diversity valley arises “from the combination of two distinct geometric mid-domain effects: geographic and thermal” (p. 184). Their thermal MDE is equivalent to our mid-environment effect. However, Brayard et al. (2005) considered the bounded spatial domain of the Atlantic basin (and thus also found a geographic MDE), while our spherical spatial domain has no equivalent to a spatial MDE. An equatorial diversity valley can also be found in the temperature-limited range-spreading model of Tomašových et al. (2015; see their fig. 1D, 1F), although they focus on latitudinal gradients in range size, not LDGs.

copepod diversity between 50°N and 60°N in the eastern Pacific (fig. 1C), although they speculated that this was “at least partly an artifact” of the particular geography of the Gulf of Alaska and the Bering Sea. If high-latitude diversity plateaus exist, they are most likely to be found for taxa with partially or wholly circumpolar ranges (fig. S3).

With respect to global LDGs, one important contrast between our model and the MDE hypothesis is that the MDE requires a bounded domain, while our model does not. Although the MDE’s logic for genuinely bounded domains may be compelling, its reliance on a boundary leaves it wanting as a purely geometric explanation for Earth’s LDG. Colwell and Hurtt’s (1994) original argument that the “northern and southern limits of habitable latitudes” constitute a domain boundary has obvious appeal, as many taxa are of course constrained to habitat below a certain latitude. However, designating polar regions as boundaries implicitly excludes polar species whose ranges occupy habitat above a certain latitude. Clearly, any explanation for global LDGs that excludes polar taxa is unsatisfying. A purely geometric hypothesis for global LDGs requires an understanding of how diversity gradients arise on a sphere without hard domain boundaries (*sensu* Colwell and Hurtt 1994), which our model provides.

On a cone, our model predicts a hump-shaped relationship between species richness and elevation, with a peak in richness closer to the base of the cone than its apex. While the large majority of published EDGs display a hump-shaped relationship (e.g., Rahbek 2005; McCain and Grytnes 2010), few published surveys have examined the precise location of the diversity peak. McCain (2009) has perhaps come closest by offering a categorization scheme for EDGs that includes low-elevation plateaus with a mid-elevation peak. While our results do not suggest a low-elevation plateau *per se*, her characterization and our model predictions both emphasize a hump-shaped EDG with greater diversity at the gradient’s base than at its apex. Our informal survey of the literature suggests that low-elevation peaks in species richness are common and can be found for such taxa as birds (Terborgh 1977; fig. 1D), ants (Bishop et al. 2014; fig. 1E), ferns (Kluge et al. 2006; fig. 1F), and fungi (Miyamoto et al. 2014). If this pattern withstands deeper scrutiny, our model provides one mechanism that could explain it.

Importantly, the cone model is concerned only with species ranges that originate on the cone itself. This may be appropriate for some scenarios, such as terrestrial species on oceanic islands. In other scenarios, such as for a terrestrial EDG, the environment at the gradient’s base may be similar to the environment of the surrounding landscape. In these cases, species with ranges that originate on the surrounding lowlands should encroach partway up the elevational gradient. Thus, we would expect species richness at low elevations to exceed the richness predicted by our

model, for the same reason that the compactness of the tropics increases diversity at low latitudes on the sphere. We have not yet found a satisfying way to incorporate this encroachment effect into our model. Nevertheless, this thinking suggests that species richness should peak at higher elevations when the base of the elevational gradient forms an ecological barrier, and at lower elevations when the base blends gradually into the surrounding landscape (Grytnes and Vetaas [2002] provide a similar result with an MDE model). In the latter case, biodiversity may even plateau at lower elevations (McCain 2009) or decline monotonically with increasing elevation if species encroachment from the surrounding landscape is strong enough.

During the review process, an interesting discussion arose regarding whether our method for constructing species ranges implicitly assumes that extreme-environment specialists possess fundamental environmental niches that extend beyond the range of existing environmental variation. Clearly, our range-construction algorithm results in narrower realized environmental niches when ranges originate near an environmental extreme, as opposed to originating at an intermediate environment, all else being equal (see Feeley and Silman 2010 for an example of a similar empirical pattern with tropical plants). However, the mathematics and predictions of our model do not depend on whether the smaller realized environmental niches of extreme-environment specialists are interpreted as truncations of larger fundamental niches or as expressions of smaller fundamental environmental niches. This distinction would be more important if the model were used to forecast how biodiversity gradients respond to environmental change (Colwell et al. 2008; Feeley and Silman 2010).

To sum up, while environmental geometry is unlikely to be the sole driver of diversity gradients, the results here suggest that even simple geometries can generate nuanced gradients in species richness when combined with basic ecological limits on species ranges. Although our comparison of model predictions with data is far from rigorous, the striking concordance between model predictions and prevailing empirical patterns suggests that the role played by geometry may be deeper and more pervasive than previously appreciated. At the very least, our results demonstrate how several pathways by which environmental geometry can impact species diversity may combine to drive fine structure in diversity gradients, and suggest relationships between this structure and ecological traits that may be profitably subjected to empirical testing. The logic of this model could also be adapted to more complex geometries, especially more realistic maps of Earth’s continental geography and/or mountain topography, although the mathematics would require a computational approach. The model could also be adapted to less conventional diversity gradients, including the microbiome of the human skin (Cos-

tello et al. 2012) or gastrointestinal tract (Stearns et al. 2011), bathymetric (depth) gradients in the ocean (Pineda and Caswell 1998), or even hypothetical diversity gradients on candidate planets for extraterrestrial life (Snyder-Beattie 2013).

Acknowledgments

This work was supported by National Science Foundation awards 08-42101, 10-15825, and 12-41794 to K.G. We thank T. Bishop, R. Colwell, R. Dunn, A. Lloyd, B. Reich, and an anonymous reviewer for useful feedback and discussion. T. Bishop and coauthors generously provided data for figure 1E. Portions of this work were completed while K.G. was on scholarly leave, hosted by C. Bergstrom and the University of Washington Department of Biology.

Literature Cited

- Barry, R. G. 2008. Mountain weather and climate. Cambridge University Press, Cambridge.
- Bertuzzo, E., F. Carrara, L. Mari, F. Altermatt, I. Rodriguez-Iturbe, and A. Rinaldo. 2016. Geomorphic controls on elevational gradients of species richness. *Proceedings of the National Academy of Sciences of the USA* 113:1737–1742.
- Bishop, T. R., M. P. Robertson, B. J. Rensburg, and C. L. Parr. 2014. Elevation-diversity patterns through space and time: ant communities of the Maloti-Drakensberg mountains of southern Africa. *Journal of Biogeography* 41:2256–2268.
- Brayard, A., G. Escarguel, and H. Bucher. 2005. Latitudinal gradient of taxonomic richness: combined outcome of temperature and geographic mid-domains effects? *Journal of Zoological Systematics and Evolutionary Research* 43:178–188.
- Brown, J. H. 2014. Why are there so many species in the tropics? *Journal of Biogeography* 41:8–22.
- Brown, J. H., G. C. Stevens, and D. M. Kaufman. 1996. The geographic range: size, shape, boundaries, and internal structure. *Annual Review of Ecology and Systematics* 27:597–623.
- Carranza, A., R. K. Colwell, and T. F. L. Rangel. 2008. Distribution of megabenthic gastropods along environmental gradients: the mid-domain effect and beyond. *Marine Ecology Progress Series* 367:193–202.
- Colwell, R. K. 2011. Biogeographical gradient theory. Pages 309–330 in S. M. Scheiner and M. R. Willig, eds. *The theory of ecology*. University of Chicago Press, Chicago.
- Colwell, R. K., G. Brehm, C. L. Cardelús, A. C. Gilman, and J. T. Longino. 2008. Global warming, elevational range shifts, and low-land biotic attrition in the wet tropics. *Science* 322:258–261.
- Colwell, R. K., N. J. Gotelli, C. Rahbek, G. L. Entsminger, C. Farrell, and G. R. Graves. 2009. Peaks, plateaus, canyons, and craters: the complex geometry of simple mid-domain effect models. *Evolutionary Ecology Research* 11:355–370.
- Colwell, R. K., and G. C. Hurtt. 1994. Nonbiological gradients in species richness and a spurious Rapoport effect. *American Naturalist* 144:570–595.
- Colwell, R. K., and D. C. Lees. 2000. The mid-domain effect: geometric constraints on the geography of species richness. *Trends in Ecology and Evolution* 15:70–76.
- Colwell, R. K., C. Rahbek, and N. J. Gotelli. 2004. The mid-domain effect and species richness patterns: what have we learned so far? *American Naturalist* 163:E1–E23.
- Colwell, R. K., and T. F. Rangel. 2010. A stochastic, evolutionary model for range shifts and richness on tropical elevational gradients under Quaternary glacial cycles. *Philosophical Transactions of the Royal Society B: Biological Sciences* 365:3695–3707.
- Connolly, S. R. 2005. Process-based models of species distributions and the mid-domain effect. *American Naturalist* 166:1–11.
- Costello, E. K., K. Stagaman, L. Dethlefsen, B. J. Bohannan, and D. A. Relman. 2012. The application of ecological theory toward an understanding of the human microbiome. *Science* 336:1255–1262.
- Crame, J. A. 2001. Taxonomic diversity gradients through geological time. *Diversity and Distributions* 7:175–189.
- Dunn, R. R., C. M. McCain, and N. J. Sanders. 2007. When does diversity fit null model predictions? scale and range size mediate the mid-domain effect. *Global Ecology and Biogeography* 16:305–312.
- Elsen, P. R., and M. W. Tingley. 2015. Global mountain topography and the fate of montane species under climate change. *Nature Climate Change* 5:772–776.
- Feeley, K. J., and M. R. Silman. 2010. Biotic attrition from tropical forests correcting for truncated temperature niches. *Global Change Biology* 16:1830–1836.
- Fischer, A. G. 1960. Latitudinal variations in organic diversity. *Evolution* 14:64–81.
- Gaston, K. J. 1996. Species-range-size distributions: patterns, mechanisms and implications. *Trends in Ecology and Evolution* 11:197–201.
- Gorelick, R. 2008. Species richness and the analytic geometry of latitudinal and altitudinal gradients. *Acta Biotheoretica* 56:197–203.
- Gotelli, N. H., and G. Graves. 1996. *Null models in ecology*. Smithsonian Institution Press, Washington, DC.
- Gross, K., and A. Snyder-Beattie. 2015. Core mathematics to support new theory for distributions of biological diversity along environmental gradients. Technical Report 2659, North Carolina State University Department of Statistics.
- Grytnes, J. A., and O. R. Vetaas. 2002. Species richness and altitude: a comparison between null models and interpolated plant species richness along the Himalayan altitudinal gradient, Nepal. *American Naturalist* 159:294–304.
- Hillebrand, H. 2004. On the generality of the latitudinal diversity gradient. *American Naturalist* 163:192–211.
- Jablonski, D., K. Roy, and J. W. Valentine. 2006. Out of the tropics: evolutionary dynamics of the latitudinal diversity gradient. *Science* 314:102–106.
- Jetz, W., and C. Rahbek. 2001. Geometric constraints explain much of the species richness pattern in African birds. *Proceedings of the National Academy of Sciences of the USA* 98:5661–5666.
- Kluge, J., M. Kessler, and R. R. Dunn. 2006. What drives elevational patterns of diversity? a test of geometric constraints, climate and species pool effects for pteridophytes on an elevational gradient in Costa Rica. *Global Ecology and Biogeography* 15:358–371.
- Lees, D. C., C. Kremen, and L. Andriamampianina. 1999. A null model for species richness gradients: bounded range overlap of butterflies and other rainforest endemics in Madagascar. *Biological Journal of the Linnean Society* 67:529–584.
- Letten, A. D., S. K. Lyons, and A. T. Moles. 2013. The mid-domain effect: it's not just about space. *Journal of Biogeography* 40:2017–2019.
- Lomolino, M. V., B. R. Riddle, R. J. Whittaker, and J. H. Brown. 2010. *Biogeography*. 4th ed. Sinauer, Sunderland, MA.

- McCain, C. M. 2004. The mid-domain effect applied to elevational gradients: species richness of small mammals in Costa Rica. *Journal of Biogeography* 31:19–31.
- . 2007. Area and mammalian elevational diversity. *Ecology* 88:76–86.
- . 2009. Global analysis of bird elevational diversity. *Global Ecology and Biogeography* 18:346–360.
- McCain, C. M., and J.-A. Grytnes. 2010. Elevational gradients in species richness. In *Encyclopedia of life sciences*. Wiley, Chichester.
- Mittelbach, G. G., D. W. Schemske, H. V. Cornell, A. P. Allen, J. M. Brown, M. B. Bush, S. P. Harrison, et al. 2007. Evolution and the latitudinal diversity gradient: speciation, extinction and biogeography. *Ecology Letters* 10:315–331.
- Miyamoto, Y., T. Nakano, M. Hattori, and K. Nara. 2014. The mid-domain effect in ectomycorrhizal fungi: range overlap along an elevation gradient on Mount Fuji, Japan. *ISME Journal* 8:1739–1746.
- Pianka, E. R. 1966. Latitudinal gradients in species diversity: a review of concepts. *American Naturalist* 100:33–46.
- Pineda, J., and H. Caswell. 1998. Bathymetric species-diversity patterns and boundary constraints on vertical range distributions. *Deep Sea Research Part II: Topical Studies in Oceanography* 45: 83–101.
- Rahbek, C. 1995. The elevational gradient of species richness: a uniform pattern? *Ecography* 18:200–205.
- . 1997. The relationship among area, elevation, and regional species richness in Neotropical birds. *American Naturalist* 149:875–902.
- . 2005. The role of spatial scale and the perception of large-scale species-richness patterns. *Ecology Letters* 8:224–239.
- Rangel, T. F. L., and J. A. F. Diniz-Filho. 2005. An evolutionary tolerance model explaining spatial patterns in species richness under environmental gradients and geometric constraints. *Ecography* 28: 253–263.
- Rangel, T. F. L., J. A. F. Diniz-Filho, and R. K. Colwell. 2007. Species richness and evolutionary niche dynamics: a spatial pattern-oriented simulation experiment. *American Naturalist* 170:602–616.
- Rohde, K. 1992. Latitudinal gradients in species diversity: the search for the primary cause. *Oikos* 65:514–527.
- Rosenzweig, M. L. 1992. Species diversity gradients: we know more and less than we thought. *Journal of Mammalogy* 73:715–730.
- . 1995. *Species diversity in space and time*. Cambridge University Press, Cambridge.
- Roy, K., D. Jablonski, J. W. Valentine, and G. Rosenberg. 1998. Marine latitudinal diversity gradients: tests of causal hypotheses. *Proceedings of the National Academy of Sciences of the USA* 95:3699–3702.
- Rutherford, S., S. D'Hondt, and W. Prell. 1999. Environmental controls on the geographic distribution of zooplankton diversity. *Nature* 400:749–753.
- Snyder-Beattie, A. E. 2013. New models for latitudinal biodiversity gradients and implications in our search for extraterrestrial life. MS thesis. North Carolina State University, Raleigh.
- Stearns, J. C., M. D. Lynch, D. B. Senadheera, H. C. Tenenbaum, M. B. Goldberg, D. G. Cvitkovitch, K. Croitoru, G. Moreno-Hagelsieb, and J. D. Neufeld. 2011. Bacterial biogeography of the human digestive tract. *Scientific Reports* 1:170.
- Terborgh, J. 1973. On the notion of favorableness in plant ecology. *American Naturalist* 107:481–501.
- . 1977. Bird species diversity on an Andean elevational gradient. *Ecology* 58:1007–1019.
- Tittensor, D. P., C. Mora, W. Jetz, H. K. Lotze, D. Ricard, E. V. Berghe, and B. Worm. 2010. Global patterns and predictors of marine biodiversity across taxa. *Nature* 466:1098–1101.
- Tomašových, A., D. Jablonski, S. K. Berke, A. Z. Krug, and J. W. Valentine. 2015. Nonlinear thermal gradients shape broad-scale patterns in geographic range size and can reverse Rapoport's rule. *Global Ecology and Biogeography* 24:157–167.
- VanDerWal, J., H. T. Murphy, and J. Lovett-Doust. 2008. Three-dimensional mid-domain predictions: geometric constraints in North American amphibian, bird, mammal and tree species richness patterns. *Ecography* 31:435–449.
- Willig, M. R., D. M. Kaufman, and R. D. Stevens. 2003. Latitudinal gradients of biodiversity: pattern, process, scale, and synthesis. *Annual Review of Ecology, Evolution, and Systematics* 34:273–309.
- Willig, M. R., and S. K. Lyons. 1998. An analytical model of latitudinal gradients of species richness with an empirical test for marsupials and bats in the New World. *Oikos* 81:93–98.
- Willig, M. R., and K. W. Selcer. 1989. Bat species density gradients in the New World: a statistical assessment. *Journal of Biogeography* 16:189–195.
- Yasuhara, M., G. Hunt, H. J. Dowsett, M. M. Robinson, and D. K. Stoll. 2012. Latitudinal species diversity gradient of marine zooplankton for the last three million years. *Ecology Letters* 15:1174–1179.

Associate Editor: Benjamin M. Bolker
Editor: Yannis Michalakos